Acta Biochimica Polonica

Vol. 53 No. 3/2006, 515–524

on-line at: www.actabp.pl

Regular paper

Novel peptide recognized by RhoA GTPase

Dominika Drulis-Fajdasz, Filip Jelen, Arkadiusz Oleksy and Jacek Otlewski✉

Department of Protein Engineering, Faculty of Biotechnology, University of Wroclaw, Wrocław, Poland;
✉e-mail: otlewski@protein.pl

Received: 04 June, 2006; revised: 29 August, 2006; accepted: 04 September, 2006
avaiable on-line: 01 October, 2006

A phage-displayed random 7-mer disulfide bridge-constrained peptide library was used to map the surface of the RhoA GTPase and to find peptides able to recognize RhoA switch regions. Several peptide sequences were selected after four rounds of enrichment, giving a high signal in ELISA against RhoA-GDP. A detailed analysis of one such selected peptide, called R2 (CWSFP-GYAC), is reported. The RhoA–R2 interaction was investigated using fluorescence spectroscopy, chemical denaturation, and determination of the kinetics of nucleotide exchange and GTP hydrolysis in the presence of RhoA regulatory proteins. All measurements indicate that the affinity of the R2 peptide for RhoA is in the micromolar range and that R2 behaves as an inhibitor of: i) GDP binding to the *apo* form of RhoA (Mg^{2+}- and nucleotide-free form of the GTPase), ii) nucleotide exchange stimulated by GEF (DH/PH tandem from PDZRhoGEF), and iii) GTP hydrolysis stimulated by the BH domain of GrafGAP protein.

Keywords: RhoA GTPase, epitope mapping, peptide phage display, PDZRhoGEF, GrafGAP

INTRODUCTION

RhoA, together with Rac1 and Cdc42, belongs to the most extensively characterized members of the Rho family of small GTPases (Paduch *et al.*, 2001). These three proteins regulate many essential cellular processes, including actin dynamics, gene transcription and cell cycle progression (Bar-Sagi & Hall, 2000). In particular, RhoA promotes actin–myosin contractility and thereby formation of stress fibres and focal adhesions responsible for the cell shape, attachment and motility. Like other molecular switches, Rho GTPases cycle between an active form, loaded with GTP, and a biologically inactive one, associated with GDP. The difference in the conformation of the two forms concerns primarily two regions, called switch I and switch II, which form the binding site for the nucleotide and a magnesium ion (Karnoub *et al.*, 2004). In the GTP-bound form, RhoA is able to interact with effectors or target molecules to initiate a downstream response.

The most important regulators of the biological activity of Rho GTPases are guanine nucleotide exchange factors (GEFs) and GTPase activating proteins (GAPs). The activation reaction requires GEFs to accelerate the release of the tightly bound GDP that is replaced by the abundant cellular GTP. Biochemical and structural data show that Dbl homology (DH) and pleckstrin homology (PH) domains are required to efficiently catalyze the GDP/GTP exchange reaction (Derewenda *et al.*, 2004). The intrinsically low hydrolysis rate of GTP by Rho GTPases can be accelerated by several orders of magnitude through association with the Bcr-homology (BH) domain of GAP proteins (Longenecker *et al.*, 2000).

Deregulated expression or over-activation of Rho GTPases have been observed in various cancers, particularly in breast carcinomas (Benitah *et al.*, 2004). For this reason, Rho GTPases are considered as potentially useful targets for therapeutic intervention. However, the precise mechanisms by which Rho GTPases participate in carcinogenesis are still poorly characterized. During the last few years in-

Abbreviations: BH, Bcr homology; CD, circular dichroism; ΔG_{den}, free energy change of denaturation; GAP, GTPase activatng protein; GdmCl, guanidinium chloride; GEF, guanine nucleotide exchange factor; GSH, reduced glutathione; GSSG, oxidized glutathione; IPTG, isopropyl β-D-1-thiogalactopyranoside; mantGDP, *N*-methylanthraniloyl-GDP; MESG, 2-amino-6-mercapto-7-methylpurine ribonucleoside; K_a, association constant; K_d, dissociation constant; PNP, purine nucleoside phosphorylase; PPD, peptide phage display.

vestigations have been focused on the exploration of small-peptide inhibitors and non-peptide chemical compounds that could selectively interact with small GTPases, GEFs or receptor proteins, thus inhibiting protein–protein interactions (Melisi *et al.*, 2004).

In this paper we applied a peptide phage display (PPD) approach to search for RhoA-specific peptides that are able to interfere with the action of the GEF and/or GAP regulatory proteins. We were able to select a disulfide bond-constrained heptapeptide, which we called R2, that bound to RhoA in the absence of magnesium ion and was able to block the exchange reaction catalyzed by the DH/PH tandem from the PDZRhoGEF regulator and to prevent the stimulation of the RhoA GTPase activity by the BH domain from the GrafGAP protein.

MATERIALS AND METHODS

Protein production and purification. A short form of the human RhoA protein was obtained, composed of 181 amino acids with the 14 C-terminal amino acids truncated, from the pET vector (Longenecker *et al.*, 2003). Three mutations G14V, Q63L and F25N were introduced to increase the protein activity and stability. The construct encoded a His-tag fusion with an rTEV protease cleavage site (Sheffield *et al.*, 1999) and the expression of the fusion protein was done in BL21(DE3)-RIL *Escherichia coli* strain (Stratagene). The cultures were grown in the LB medium at 37°C. Expression of the protein was induced at OD_{600} of about 0.4 to 0.6 with 0.5 mM IPTG. The culture was grown at 37°C for further 4 h. Cell pellet was resuspended in lysis buffer (50 mM Tris, 400 mM NaCl, 5 mM $MgCl_2$, 5 mM imidazole, pH 8.0) and disrupted by sonication. The soluble protein fraction was purified by binding to an Ni-NTA-agarose column (Qiagen) and eluted with 50 mM Tris, 150 mM NaCl, 5 mM $MgCl_2$, 150 mM imidazole, pH 8.0. The His-tag was removed by digestion with rTEV protease at 10°C for 36 h and dialysis against cleavage buffer (Kapust *et al.*, 2001). Subsequently, RhoA was purified by rechromatography on Ni-NTA-agarose to remove the His-tag and undigested RhoA-6×His protein (25 mM Tris, 5 mM $MgCl_2$, 10 mM β-mercaptoethanol, pH 8.0). To uniformly replace the physiologically bound nucleotide (GDP or GTP) with GDP, the protein was incubated for 1 h with 10 mM EDTA and 10 mM GDP. The reaction was terminated by addition of 20 mM $MgCl_2$, and the remaining nucleotide, as well as EDTA, were removed on a desalting column (Qiagen) (equilibrated in 25 mM Tris, 150 mM NaCl, 5 mM $MgCl_2$, pH 8.0). Cdc42 and Rac1 GTPase proteins were prepared applying exactly the same protocol.

Preparation of metal ion- and nucleotide-free *apo*GTPase. To remove Mg^{2+} and nucleotide bound to the GTPase (RhoA, Cdc42 or Rac1), a purified protein sample (about 100 μM) was incubated with EDTA at 10°C for 3 h (EDTA was in a 4-fold molar excess over Mg^{2+} concentration). Then, the protein was desalted on a column equilibrated with 10 mM Hepes, 25 mM NaCl, pH 7.4. The *apo*GTPase (*apo*RhoA, *apo*Cdc42 and *apo*Rac1) was kept at 4°C at a low concentration (about 9 μM) to avoid protein precipitation. To examine the content of the nucleotide remaining in the protein sample, UV absorption spectra of the EDTA-treated samples were recorded in the 240 to 300 nm range and compared with a GTPase sample that was not treated with EDTA. A lack of the GDP maximum at 254 nm confirmed that the sample was in the *apo* form.

Screening of a phage-displayed random peptide library. We used three filamentous phage libraries: 12-mer and a 7-mer linear peptide libraries, and a 7-mer disulfide bridge-constrained peptide library (Ph.D.-12, Ph.D.-7 and Ph.D.-C7C™ Peptide Library Kit, respectively, from NEB), to select for peptides recognizing RhoA (Fack *et al.*, 1997). The selection was performed according to a manual supplied by NEB. In brief, MaxiSorp plates were coated with 100 μl of RhoA-GDP protein (100 μg/ml, overnight at 4°C) in a buffer containing low concentration of Mg^{2+} (25 mM Tris, 150 mM NaCl, 0.25 mM $MgCl_2$, pH 7.4, hereafter called Tris buffer). The wells were blocked with 300 μl of 1% BSA in Tris buffer for 2 h at room temperature. Diluted phages (2×10^{10} pfu) in Tris-buffer containing 0.1% BSA were added to the RhoA-GDP-coated wells and rocked gently for 3 h at room temperature. Unbound and weakly bound phages were discarded by washing 50 times with Tris buffer containing 0.05% Tween 20. Bound phages were eluted by incubation with 100 μl of 0.2 M glycine/HCl, pH 2.2, for 10 min and neutralized with 1 M Tris (pH 8.5). The eluted phages were amplified in *E. coli* strain ER2738 (NEB). Four rounds of selection were performed and each time the titre of the eluted phages was determined by plaque forming assay to verify the enrichment factor of the selected library in comparison to the control (BSA-coated wells). Eluted phages were titered and amplified.

Phage ELISA. Unique phage clones were obtained and phage ELISA was performed according to the NEB manual for the library. Briefly, a 96-well immunoplate (MaxiSorp NUNC, USA) was coated with 100 μl of RhoA-GDP protein (4 μg/ml) overnight at 4°C, then blocked with 1% BSA in PBS for 2 h at room temperature. Individual phage clones, suspended in PBS containing 0.1% BSA, were added to immunoplate wells and incubated for 1 h at room temperature. Afterwards the plate was incubated for an additional 1 h with horseradish peroxidase-con-

jugated anti-M13 antibodies (Pharmacia) (1:5000, PBS, 0.1% BSA). After each incubation the plate was washed ten times with PBS containing 0.05% Tween 20. Reaction was developed with *ortho*-phenylenediamine as the chromogene in a 0.1 M Na-citrate buffer (pH 4.5) and 0.01% H_2O_2 and quantitated at $\lambda = 490$ nm using a SpectraMax 340 Microplate Spectrophotometer (Molecular Devices). DNA of the selected clones was isolated using QIAprepSpin Miniprep Kit (Qiagen) from infected bacteria and sequenced.

Peptide purification. Crude peptides (R2 and R3) were purchased from BioSynthesis (Lewisville, USA) and purified before and after cyclization by reversed-phase HPLC (Waters) using a C_{18} column (218TP518, Vydac) and 0.1% trifluoroacetic acid (TFA) / 100% acetonitrile (ACN) gradient. Peptides (0.1 mg/ml) were cyclized overnight at 11°C in 0.1 M Tris-buffer containing 4 M urea, 300 nM GSSH, 150 nM GSH, 3 mM EDTA (pH 8.7). The identity of the peptides was verified by electrospray mass spectrometry.

Binding of R2 to *apo*RhoA. *Apo*RhoA (0.7 μM) was pre-incubated with increasing concentrations of R2 (10 nM–50 μM R2 peptide in Hepes, 25 mM NaCl, pH 7.4) at 10°C for 3 h, and then 1 μM mantGDP was added. After equilibrium was reached, the fluorescence intensity of mantGDP incorporated into RhoA was monitored ($\lambda_{ex} = 356$ nm, $\lambda_{em} = 445$ nm) using a SpectraMax GEMINI-XS Microplate Spectrofluorometer (Molecular Devices). Fluorescence signals were recalculated for free *apo*RhoA concentration (B) and plotted against total R2 concentration (P). Data were fitted to Eqn. 1 to derive the K_a value for R2–*apo*RhoA association:

$$B = 0.5^* (B_o - P - 1/K_a + \mathrm{Sqrt}((B_o + P + 1/K_a)^2 - 4^*B_o^*P)) \quad (1)$$

where B_o is the total RhoA concentration in the absence of R2 peptide; and converted to obtain K_d:

$$K_d = 1/K_a \quad (2)$$

In parallel we tested the interaction between R2 and *apo*Cdc42, and R2 and *apo*Rac1.

Chemical denaturation. The denaturation studies were carried out in two separate series: in the Mg^{2+}-containing buffer A (10 mM Tris, 100 mM NaCl, 5 mM $MgCl_2$, 0.1 mM GDP, pH 7.4), or in the Mg^{2+}-free buffer B (10 mM Na_2HPO_4, 100 mM NaCl, 0.1 mM GDP, pH 7.4), as described in (Thapar *et al.*, 2002). RhoA was diluted to a final concentration of 2.5 μM, and the peptide was present in a 3- to 20-fold molar excess relative to the protein. All samples were incubated at 20°C for 1 h prior to data collection. A Jasco J-715 spectropolarimeter equipped with a Jasco 2 Syringe Titrator was used to obtain complete guanidinium hydrochloride (GdmCl) denaturation curves. The samples were placed in a 1 cm quartz cuvette, and the ellipticity was recorded as a function of time at 224 nm. To calculate the dissociation constant for the binding of R2 to native RhoA we adopted a method described by Meiering *et al.* (1991). It was assumed that the peptide binds to a single binding site in the native GTPase:

$$NP \Leftrightarrow N + P \Leftrightarrow D + P \quad (3)$$

where N is the native protein, NP is the native protein–peptide complex, P is the peptide, D is the denatured protein, and

$$K_u = [D]/[N] \quad (4)$$
$$K_d = [N][P]/[NP] \quad (5)$$
$$K_u^P = [D]/([N] + [NP]) \quad (6)$$

where K_u is the equilibrium constant of protein unfolding, K_u^P is the apparent equilibrium constant of unfolding in the presence of peptide, and K_d is the native protein–peptide dissociation constant. Denaturation data were fitted to the equation described by Santoro and Bolen (1992):

$$\theta = \frac{a_n + b_n[GdmCl] + a_u + b_u[GdmCl]\exp\frac{m[GdmCl] - \Delta G_{den}^{H_2 0}}{RT}}{1 + \exp\frac{m[GdmCl] - \Delta G_{den}^{H_2 0}}{RT}} \quad (7)$$

where a_n and a_u are the intercepts of the respective base lines before and after unfolding, b_n and b_u are the respective slopes of the pre- and posttransition base lines, $[GdmCl]$ is the molar concentration of denaturant, m is the slope of the linearized data in the transition region, ΔG is the apparent free energy of unfolding in the absence of denaturant, R is the gas constant (1.98 cal mol^{-1} K^{-1}), T is the absolute temperature (298 K) and exp denotes exponent. The values of m and ΔG were used to calculate the K_u and K_u^P:

$$K_u^P = \exp[m\,[G50] - (\Delta G)/(RT)] \quad (8)$$

The K_d was then calculated from the slope of the K_u/K_u^P *vs.* peptide concentration plot, according to Eqn. 9:

$$K_u/K_u^P = 1 + [P]/K_d \quad (9)$$

Guanine nucleotide exchange assay. To determine whether R2 prevents the GDP/mantGDP exchange reaction catalyzed by the DH/PH tandem from the PDZRhoGEF protein, the time course of the fluorescence changes resulting from the GDP→

mantGDP exchange stimulated by 0.1 mM DH/PH was recorded in the presence of increasing concentrations of R2 (from 0.5 to 60 μM). Peptide R2 and 0.5 μM RhoA were pre-incubated at 10°C for 3 h (10 mM Hepes, 25 mM NaCl, 0.1 mM EDTA, pH 7.5). The nucleotide exchange reaction was then initiated by addition of 5 mM Mg^{2+}, 1 μM mantGDP and 0.1 mM DH/PH. Total fluorescence intensities of mantGDP incorporated into RhoA were measured in a 1 cm cuvette using a Jasco FP-750 fluorimeter. The fluorescence signals from mantGDP were converted to free RhoA concentration and plotted against the total R2 concentration. The dissociation constant was calculated using Eqns. 1 and 2.

GAP-stimulated GTP hydrolysis. The influence of R2 on the kinetics of GAP-stimulated GTP hydrolysis was based on a MESG/phosphorylase assay (Webb, 1992). The BH domain from the GrafGAP protein (GTPase regulator associated with FAK), an activator of both RhoA and Cdc42 GTPases, was used. In the presence of EDTA, RhoA catalyzes multiple turnover reaction of GTP hydrolysis resulting in a linear rate of γP_i release (Zhang *et al.*, 1997). The R2 peptide (0.4 μM to 200 μM) was preincubated with RhoA at 10°C for 3 h. The activity of 5 mM RhoA (in 50 mM Hepes, 0.1 mM EDTA, 100 mM GTP, 100 μM MESG, 5 U of coupling phosphorylase and 0.02 mM BH-domain, pH 7.8) was followed by measuring the absorbance changes at 360 nm. Samples were kept in a thermostated cell holder at 20°C and the reaction progress was recorded on a Cary 3e spectrophotometer (Varian, USA). The rates of hydrolysis were converted to free RhoA concentrations and plotted against total R2 peptide concentrations to calculate the dissociation constant (Eqns 1. and 2).

RESULTS

Affinity selection

An analysis of the 26 known structures of complexes of Rho GTPases with their protein regulators and effectors shows that these interacting partners recognize different surfaces of the GTPases (Corbett & Alber, 2001). The binding epitopes, however, always include a common set of conserved amino acids that are clustered on the surface of the switch regions (Corbett & Alber, 2001; Dvorsky & Ahmadian, 2004). It appears that the switch regions were selected during evolution to interact with effectors for functional reasons. To address the question whether one can identify peptides able to recognize the switches and to disrupt the interaction with the RhoA partner proteins we performed a phage display selection on RhoA using three different libraries: a 12-mer and a 7-mer linear peptide libraries, and a 7-mer disulfide bridge-constrained peptide library (Ph.D.-12, Ph.D.-7 and Ph.D.-C7C Peptide Library Kit, NEB) (Fack *et al.*, 1997). Peptides were presented pentavalently on the surface of M13 bacteriophage in the form of amino-terminal fusions to the pIII protein (Sidhu, 2001). All three libraries were unbiased, thus it should be possible to select peptides for any part of RhoA surface.

Table 1. Amino-acid sequences of Rho-binding peptides selected from the Ph.D.-C7C random peptide library.

Clone	Sequence	Frequency	δA*
R1	C-TLCYMEC-C	4	5.8
R2	**C-WSFPGYA-C**	**2**	**5.6**
R3	C-NYVGSHA-C	6	2.5
R4	C-SITMRAN-C	2	2.0
R5	C-SLVPMRA-C	1	2.8
R6	C-STHIKKT-C	1	2.3

*ELISA reactivity — δA is the ratio of A_{490} obtained for RhoA and A_{490} obtained for control (BSA).

The GDP-bound form of RhoA was used for affinity selection, since GTP is hydrolyzed too quickly by the GTPase to ensure stable selection conditions. In our initial selection attempts 5 mM $MgCl_2$ was added to stabilize the conformation of switch I and II regions. However, we did not observe an enrichment of the pool of phages up to the fifth round of selection. When individual clones were sequenced after the third, fourth or fifth selection round, no domination of any single or consensus sequence could be observed. Therefore, we significantly lowered the magnesium concentration for the other selection approach, since it is known from a comparison of the respective crystal structures (Wei *et al.*, 1997; Shimizu *et al.*, 2000) that in the absence of Mg^{2+} switch I is completely removed from the nucleotide-binding site. Less pronounced conformational changes occur also in switch II as its 3_{10}-helix H1 (residues 64 to 66) forms a β-turn in the absence of Mg^{2+} (Shimizu *et al.*, 2000). During selection $MgCl_2$ was kept at 0.25 mM, since at lower concentrations RhoA showed a pronounced tendency to precipitate.

Four rounds of affinity selection were applied to the three peptide libraries under these conditions. The disulfide bond-constrained library, but not the two linear peptide libraries, were enriched after four rounds of selection. Therefore, using phage ELISA we further analyzed only clones selected from the constrained library. The results showed that 90% of randomly picked phage clones were positive in

the ELISA and bound to RhoA. These clones were characterized by DNA sequencing (Table 1). We did not analyze further the R1 clone since its peptide contained four cysteines and it was hard to identify their pairings on the phage surface. Regarding clone R3 we found that corresponding synthetic peptide did not bind to RhoA and did not affect either PDZRhoGEF or GrafGAP binding (not shown). We also did not analyze clones R4, R5 and R6 as they showed relatively weak signals in the ELISA and, in addition, clones R5 and R6 were poorly represented in the selected phage pool (Table 1).

Inhibition of nucleotide binding to *apo*RhoA

Unlike the Ras and Rab proteins, Rho GTPases bind GTP or GDP with the same affinity independently of Mg^{2+}. The magnesium ion acts solely to stabilize the bound GTP or GDP by equally slowing down the off and on rate constants (Zhang *et al.*, 2000).

To measure the binding affinity of R2 for the nucleotide- and magnesium-free form of RhoA (*apo*RhoA), we applied spontaneous incorporation of mantGDP to *apo*RhoA in the presence of increasing concentrations of R2 peptide. The experiment was performed at a low temperature due to the instability of *apo*RhoA. Preincubation of *apo*RhoA with the R2 peptide at 10°C and subsequent addition of mantGDP led to a decreased fluorescence signal (relative to such a signal in the absence of R2) indicating that R2 blocked GDP binding to RhoA. The fluorescence data were recalculated (as described in Materials and Methods) to determine the dissociation constant (Fig. 1A). The K_d value was found to be 13.3 μM. When similar experiments were performed using *apo*Cdc42 and *apo*Rac1 no R2-dependent changes in fluorescence signal were observed indicating that R2 did not affect the binding of mantGDP to the *apo* form of these GTPases.

We also studied whether the R2 peptide can displace mantGDP from RhoA-mantGDP. Rather surprisingly, addition of R2 to a preformed RhoA–mantGDP complex did not cause any changes in the fluorescence on a 20 min time scale (not shown). Since the dissociation rate constant (k_{off}) of the RhoA–GDP complex is 1.4 min^{-1} (Zhang *et al.*, 2000), the incubation time was sufficient to allow for the substitution of mantGDP with the peptide. Based on this experiment, we conclude that R2 cannot displace mantGDP from the RhoA binding pocket. On the other hand, binding of R2 to RhoA prevents association between mantGDP and the GTPase.

Binding and specificity of R2 peptide to RhoA — a chemical denaturation study

To further analyze the R2–RhoA interaction, we performed denaturation of RhoA in the presence of increasing R2 peptide concentrations. In principle, an increase of protein stability in the presence of a ligand indicates protein–ligand complex formation.

We could not analyze denaturation of *apo*RhoA since it is extremely unstable and aggregates rapidly at room temperature and/or higher concentration. Moreover, thermal unfolding parameters of RhoA-GDP could not be determined due to irreversible aggregation of the protein at temperatures above the midpoint of transition. Instead, we applied chemical denaturation to study the RhoA stability in the presence of the ligand.

In particular, we studied GdmCl-induced denaturation of free RhoA-GDP and RhoA-GDP in the presence of R2 peptide, followed by circular dichroism signal at 224 nm, in the presence or absence of Mg^{2+}. Figure 2A shows the respective denatura-

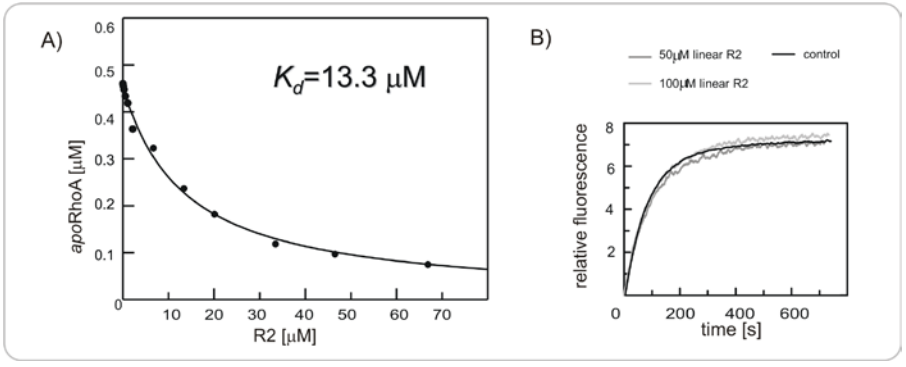

Figure 1. Binding of R2 peptide to *apo*RhoA.
(A) Determination of the dissociation constant for the R2–*apo*RhoA complex. The total fluorescence intensity of mantGDP (λ_{ex} = 356 nm, λ_{em} = 445 nm) incorporated into RhoA GTPase was recalculated to give free *apo*RhoA concentration which was then plotted *versus* R2 peptide concentration. The curve displayed was fitted to the data by Eqns. 1 and 2. (B) Binding of mantGDP to the *apo*RhoA protein in the absence (control) and presence of the linear (reduced) form of R2 peptide at 50 and 100 μM concentration. No influence of the reduced R2 peptide on GDP binding to *apo*RhoA was observed.

Table 2. Thermodynamic parameters for GdmCl-induced denaturation of RhoA-GDP and Cdc42-GDP in the absence and presence of 25 μM R2 peptide.

	buffer A (with Mg^{2+})			buffer B (without Mg^{2+})		
	$[GdmCl]_{50}$ [M]	ΔG [cal mol^{-1} M^{-1}]	m [cal mol^{-1}]	$[GdmCl]_{50}$ [M]	ΔG [cal mol^{-1} M^{-1}]	m [cal mol^{-1}]
RhoA-GDP	0.7	4130	6064	0.77	4710	5927
R2:RhoA-GDP	0.71	4080	5680	**0.83**	**7052**	**8425**
Cdc42-GDP	2.7	5436	2012	2.68	7423	2767
R2:Cdc42-GDP	2.66	5502	2064	2.65	7600	2870

tion curves in the absence of magnesium ion. Stabilization of RhoA due to R2 peptide binding was observed in a buffer without Mg^{2+}, but not in the presence of 5 mM $MgCl_2$ (Table 2). Additionally, both the GTPase and the R2–GTPase complex display cooperative denaturation behaviour (Burke *et al.*, 1993).

To calculate the dissociation constant (K_d) for the R2–RhoA-GDP complex we applied a method described by Meiering *et al.* (1991) and determined denaturation curves in the presence of 10 μM and 25 μM R2 peptide. K_u/K_u^P (the ratio of denaturation constant in the absence and presence of peptide) varies linearly with the peptide concentration and the value of K_d (30 μM) could be calculated from the slope of the plot (Fig. 2B). The linearity of this plot further suggests a one-to-one stoichiometry of the R2–RhoA interaction (Sancho *et al.*, 1991). We did not observe an R2-induced stabilization of Cdc42 (Table 2), which suggests that R2 is rather specific towards RhoA.

Inhibition of GEF-stimulated guanine nucleotide exchange in RhoA

We showed above that R2 peptide can block the binding of GDP to RhoA and that this peptide stabilizes the Rho–GDP complex. This suggests that R2 recognizes RhoA in the vicinity of the switch regions. Thus it appeared plausible that R2 can affect the binding of protein regulators of RhoA, such as guanine nucleotide exchange factors (GEFs) or GTPase activating proteins (GAPs), since both types of regulators recognize the surface of the switch I and II regions.

To test whether R2 peptide can block the GEF-catalyzed GDP-mantGDP exchange reaction on RhoA we used the DH/PH tandem from the PZDRhoGEF protein which has been shown to selectively catalyze the nucleotide exchange on RhoA (Derewenda *et al.*, 2004). In the experiment we measured the exchange of RhoA-bound GDP for mantGDP that was present in a 2-fold excess in the reaction solution. It can be easily noticed from the plots of the time dependence of fluorescence intensity that increasing concentrations of R2 decrease the extent of mantGDP binding (Fig. 3A). Total fluorescence intensities of mantGDP bound to the GTPase were recalculated to obtain concentration of free RhoA, which was then plotted *versus* total R2 concentration (Fig. 3B). The calculated dissociation constant (13.2 μM) is in good agreement with those determined from the inhibition of mant-GDP binding and the denaturation study. These results indicate that the GEF-RhoA complex formation

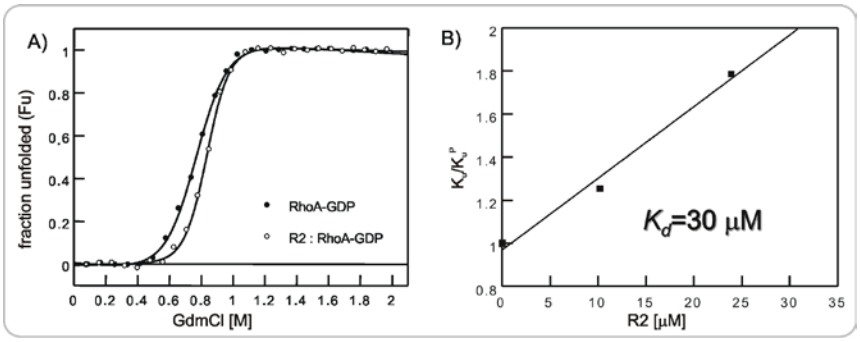

Figure 2. Determination of the dissociation constant for the R2–RhoA-GDP complex in chemical denaturation assay.
A) GdmCl denaturation of free RhoA (•) and in the presence of a 10-fold molar excess of R2 peptide (o). Circular dichroism (CD) data were normalized and presented as the fraction of unfolded protein (F_u) plotted *versus* GdmCl concentration. The data points were fitted using Eqn. 7. B) Dependence of K_u/K_u^P for RhoA-GDP on the R2 peptide concentration (buffer without Mg^{2+}). The linear plot indicates that there is one peptide binding site in the native protein. The slope of the plot equals $1/K_d$.

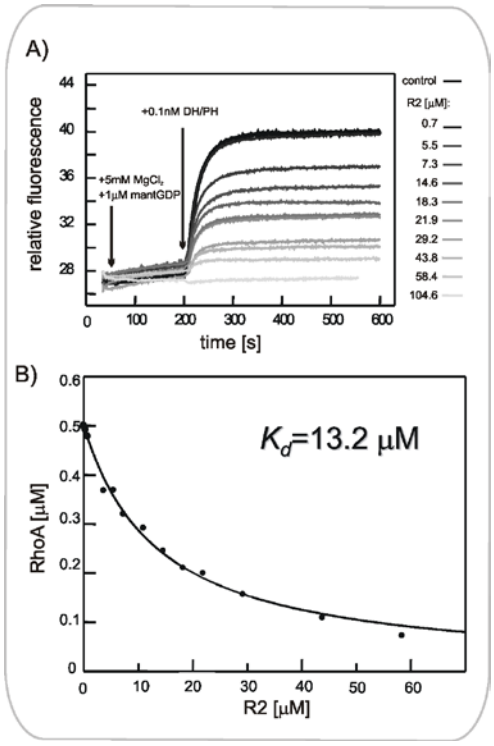

Figure 3. Determination of the dissociation constant for the R2–RhoA-GDP complex in guanine nucleotide exchange assay.
(A) The exchange reaction was monitored by measuring the increase in the mantGDP fluorescence intensity as a result of its incorporation into RhoA. At the indicated time (*arrows*), Mg^{2+}, mantGDP and DH/PH were added to initiate the exchange reaction in RhoA preincubated with R2. (B) The total fluorescence intensity of mantGDP (λ_{ex} = 356 nm, λ_{em} = 445 nm) was recalculated to give free RhoA concentration and plotted *versus* total R2 peptide concentration. The curve is the best fit to experimental data applying Eqns. 1 and 2.

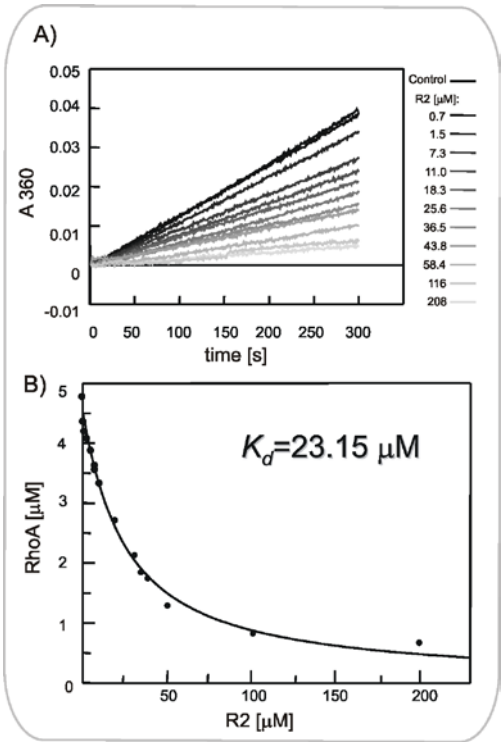

Figure 4. Determination of the dissociation constant for the R2–RhoA complex in GAP-stimulated GTP-hydrolysis assay.
(A) γP_i released from RhoA-bound GTP was measured by continuous MESG/PNP spectroscopic assay, as described in Materials and Methods. The initial slopes of GTP hydrolysis were fitted into a linear equation to give the rate constants for EDTA-induced multiple turnover reactions. Hydrolysis was monitored for 5 μM RhoA preincubated with peptide R2. (B) The dissociation rate constant for GAP-induced multiple turnover reaction was recalculated to give free RhoA concentration for each sample and plotted *versus* R2 peptide concentration. The curve displayed was fitted to the data by Eqns. 1 and 2 to give the K_d value.

and, consequently, the GEF-catalyzed nucleotide exchange is blocked by R2. Due to the much lower activity of the DH/PH tandem towards Cdc42 (Derewenda *et al.*, 2004) we were unable to determine whether R2 peptide can block the exchange reaction for this GTPase as well.

Inhibition of GAP-stimulated GTP hydrolysis by RhoA

Finally, we tested whether the R2 peptide can block GAP-stimulated GTP hydrolysis. We used an isolated GAP domain from the Graf protein that is selective towards RhoA and Cdc42 (Hildebrand *et al.*, 1996). We applied a continuous spectroscopic assay of γP_i release from the RhoA–GTP complex quantified with the MESG reaction (Zhang *et al.*, 1997). In the presence of 0.1 mM EDTA the GAP-catalyzed GTP hydrolysis reaction obeys multiple turnover kinetics resulting in a linear rate of γP_i release (Fig. 4A). The initial rates of the reaction measured at increasing concentrations of R2 peptide were recalculated to give free RhoA concentration and plotted against R2 concentration (Fig. 4B). The data were fitted by non-linear regression (Eqns. 1 and 2) to calculate the dissociation constant for the RhoA–R2 interaction. Again, the K_d (23.15 μM) is in good agreement with the results of the previously performed experiments. Since GrafGAP is also effective against Cdc42, we checked whether R2 could also block this reaction. However, no effect was observed up to 0.2 mM concentration of R2 (not shown).

DISCUSSION

Phage-displayed peptide libraries (PPD) have become an important tool in the identification of peptide ligands of a large variety of protein targets (Ladner *et al.*, 2004). To map the surface of RhoA GTPase we initially tested three different libraries: a linear dodecapeptide, a linear heptapep-

tide, and a cyclic heptapeptide library. We were able to select positive clones from the heptapetide cyclic library but not from either of the linear libraries. This is in general agreement with earlier studies showing that peptides recognizing protein surfaces can be more efficiently selected from disulfide-constrained libraries due to the stabilization of the peptide conformation imposed by the S-S bridge (Sidhu, 2000; Sidhu *et al.*, 2000; Deshayes *et al.*, 2002).

We presented a detailed analysis for one of the selected cyclic peptides (R2, CWSFPGYAC). This peptide recognizes RhoA only in its oxidized state, as blocking of its thiol groups with TCEP abolishes its binding to RhoA (Fig. 1b). Our data show that R2 recognizes RhoA only in the absence of Mg^{2+}. The crystal structure of the Mg^{2+}-free form of RhoA indicates that the loss of magnesium induces a large conformational change: switch I moves far from the nucleotide-binding site thus opening entrance to the pocket (Fig. 5) (Shimizu *et al.*, 2000). It is thus reasonable to speculate that the R2 peptide covers the nucleotide binding site. We showed that R2 prevents mantGDP binding to RhoA (but not to Cdc42 or Rac1) and stabilizes the RhoA–GDP complex against chemical denaturation.

Since our data suggest that R2 binds in the vicinity of the nucleotide binding pocket we asked whether the peptide interferes with the binding of regulatory proteins to RhoA. We chose the DH/PH tandem from PDZRhoGEF (Jelen *et al.*, 2003; Derewenda *et al.*, 2004) and the BH domain from GrafGAP (Longenecker *et al.*, 2000) that both recognize the switch regions of RhoA. Tests on the DH/PH and BH domains proved that R2 could effectively block the nucleotide exchange reaction induced by the DH/PH tandem and the GTP hydrolysis accelerated by BH. The R2 peptide binds to RhoA but not to Cdc42, as it does not interfere with the BH-stimulated GTP hydrolysis by Cdc42. Whether R2 peptide is able to distinguish among RhoA and its close homologs, RhoB and RhoC, remains to be investigated.

A survey of the literature reveals that binding sites for phage-derived peptides overlap with the binding sites for natural ligands. It has also been noted that phage display methods tend to identify 'hot spots' on proteins that form energetically critical contacts in a protein–protein interaction (Fairbrother *et al.*, 1998; Sidhu *et al.*, 2003). These observations suggest that protein binding sites have physical properties that predispose them to ligand binding (Cochran, 2001; Arkin & Wells, 2004). Blocking of GDP binding, together with inhibition of the DH/PH and BH catalyzed reactions show that R2 obeys these general selection rules.

Only a few compounds are known that are able to influence the signalling pathways involving GTPases. They were discovered by virtual library screening (Gao *et al.*, 2004), two-hybrid system screening (Kato-Stankiewicz *et al.*, 2002; Schmidt *et al.*, 2002) or phage display selection (Murase *et al.*, 2003). The R2 peptide constitutes a novel Rho-specific small-molecule inhibitor that could be used to study the role of RhoA in various cellular functions and to attempt reversing the tumour cell phenotypes associated with RhoA overactivation.

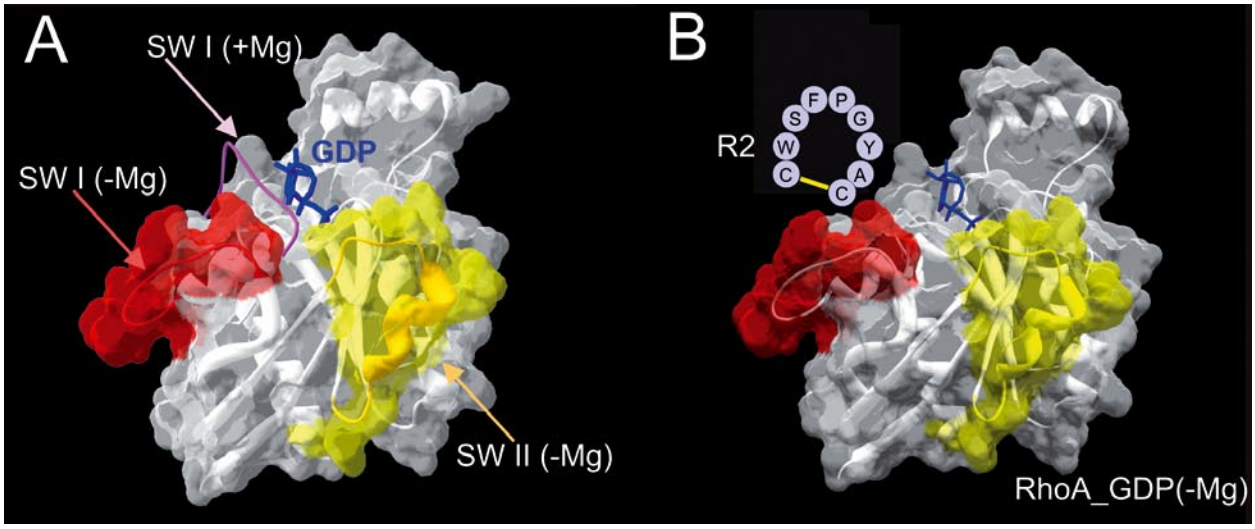

Figure 5. The suggested mode of interaction between RhoA-GDP and R2 peptide.
(A) Superimposition of RhoA-GDP-Mg^{2+} (PDB code 1FTN) and RhoA-GDP magnesium free (PDB code 1DPF) structures shows differences in the switch regions conformation. Color coding: yellow, switch region II; red and pink, switch I in the absence and in the presence of magnesium ion, respectively; blue, GDP molecule. (B) The crystal structure of the Mg^{2+}-free form of RhoA-GDP (PDB code 1DPF) with the suggested location of the R2 peptide. Note that R2 is not in scale of RhoA structure.

Acknowledgements

This work was supported by a grant 2P04A05626 from the Polish Ministry of Science and Higher Education. The authors would like to thank Dr. Zygmunt Derewenda for generously providing expression vectors for RhoA, Cdc42 and Rac1 proteins. Filip Jelen was supported by a young scientist fellowship from the Foundation for Polish Science.

REFERENCES

Arkin MR, Wells JA (2004) Small-molecule inhibitors of protein-protein interactions: progressing towards the dream. *Nat Rev Drug Discov* **3**: 301–317.

Bar-Sagi D, Hall A (2000) Ras, Rho GTPases: a family reunion. *Cell* **103**: 227–238.

Benitah SA, Valeron PF, van Aelst L, Marshall CJ, Lacal JC (2004) Rho GTPases in human cancer: an unresolved link to upstream, downstream transcriptional regulation. *Biochim Biophys Acta* **1705**: 121–132.

Burke CJ, Volkin DB, Mach H, Middaugh CR (1993) Effect of polyanions on the unfolding of acidic fibroblast growth factor. *Biochemistry* **32**: 6419–6426.

Cochran AG (2001) Protein-protein interfaces: mimics, inhibitors. *Curr Opin Chem Biol* **5**: 654–659.

Corbett KD, Alber T (2001) The many faces of Ras: recognition of small GTP-binding proteins. *Trends Biochem Sci* **26**: 710–716.

Derewenda U, Oleksy A, Stevenson AS, Korczynska J, Dauter Z, Somlyo AP, Otlewski J, Somlyo AV, Derewenda ZS (2004) The crystal structure of RhoA in complex with the DH/PH fragment of PDZRhoGEF, an activator of the Ca(2+) sensitization pathway in smooth muscle. *Structure (Camb)* **12**: 1955–1965.

Deshayes K, Schaffer ML, Skelton NJ, Nakamura GR, Kadkhodayan S, Sidhu SS (2002) Rapid identification of small binding motifs with high-throughput phage display: discovery of peptidic antagonists of IGF-1 function. *Chem Biol* **9**: 495–505.

Dvorsky R, Ahmadian MR (2004) Always look on the bright site of Rho: structural implications for a conserved intermolecular interface. *EMBO Rep* **5**: 1130–1136.

Fack F, Hugle-Dorr B, Song D, Queitsch I, Petersen G, Bautz EK (1997) Epitope mapping by phage display: random versus gene-fragment libraries. *J Immunol Methods* **206**: 43–52.

Fairbrother WJ, Christinger HW, Cochran AG, Fuh G, Keenan CJ, Quan C, Shriver SK, Tom JY, Wells JA, Cunningham BC (1998) Novel peptides selected to bind vascular endothelial growth factor target the receptor-binding site. *Biochemistry* **37**: 17754–17764.

Gao Y, Dickerson JB, Guo F, Zheng J, Zheng Y (2004) Rational design, characterization of a Rac GTPase-specific small molecule inhibitor. *Proc Natl Acad Sci USA* **101**: 7618–7623.

Hildebrand JD, Taylor JM, Parsons JT (1996) An SH3 domain-containing GTPase-activating protein for Rho, Cdc42 associates with focal adhesion kinase. *Mol Cell Biol* **16**: 3169–3178.

Jelen F, Oleksy A, Smietana K, Otlewski J (2003) PDZ domains — common players in the cell signaling. *Acta Biochim Polon* **50**: 985–1017.

Kapust RB, Tozser J, Fox JD, Anderson DE, Cherry S, Copeland TD, Waugh DS (2001) Tobacco etch virus protease: mechanism of autolysis, rational design of stable mutants with wild-type catalytic proficiency. *Protein Eng* **14**: 993–1000.

Karnoub AE, Symons M, Campbell SL, Der CJ (2004) Molecular basis for Rho GTPase signaling specificity. *Breast Cancer Res Treat* **84**: 61–71.

Kato-Stankiewicz J, Hakimi I, Zhi G, Zhang J, Serebriiskii I, Guo L, Edamatsu H, Koide H, Menon S, Eckl R, Sakamuri S, Lu Y, Chen QZ, Agarwal S, Baumbach WR, Golemis EA, Tamanoi F, Khazak V (2002) Inhibitors of Ras/Raf-1 interaction identified by two-hybrid screening revert Ras-dependent transformation phenotypes in human cancer cells. *Proc Natl Acad Sci USA* **99**: 14398–14403.

Ladner RC, Sato AK, Gorzelany J, de Souza M (2004) Phage display-derived peptides as therapeutic alternatives to antibodies. *Drug Discov Today* **9**: 525–529.

Longenecker KL, Zhang B, Derewenda U, Sheffield PJ, Dauter Z, Parsons JT, Zheng Y, Derewenda ZS (2000) Structure of the BH domain from graf, its implications for Rho GTPase recognition. *J Biol Chem* **275**: 38605–38610.

Longenecker K, Read P, Lin SK, Somlyo AP, Nakamoto RK, Derewenda ZS (2003) Structure of a constitutively activated RhoA mutant (Q63L) at 1.55 A resolution. *Acta Crystallogr D Biol Crystallogr* **59**: 876–880.

Meiering EM, Bycroft M, Fersht AR (1991) Characterization of phosphate binding in the active site of barnase by site-directed mutagenesis, NMR. *Biochemistry* **30**: 11348–11356.

Melisi D, Troiani T, Damiano V, Tortora G, Ciardiello F (2004) Therapeutic integration of signal transduction targeting agents, conventional anti-cancer treatments. *Endocr Relat Cancer* **11**: 51–68.

Murase K, Morrison KL, Tam PY, Stafford RL, Jurnak F, Weiss GA (2003) EF-Tu binding peptides identified, dissected, affinity optimized by phage display. *Chem Biol* **10**: 161–168.

Paduch M, Jelen F, Otlewski J (2001) Structure of small G proteins and their regulators. *Acta Biochim Polon* **48**: 829–850.

Sancho J, Meiering EM, Fersht AR (1991) Mapping transition states of protein unfolding by protein engineering of ligand-binding sites. *J Mol Biol* **221**: 1007–1014.

Santoro MM, Bolen DW (1992) A test of the linear extrapolation of unfolding free energy changes over an extended denaturant concentration range. *Biochemistry* **31**: 4901–4907.

Schmidt S, Diriong S, Mery J, Fabbrizio E, Debant A (2002) Identification of the first Rho-GEF inhibitor, TRIPalpha, which targets the RhoA-specific GEF domain of Trio. *FEBS Lett* **523**: 35–42.

Sheffield P, Garrard S, Derewenda Z (1999) Overcoming expression, purification problems of RhoGDI using a family of "parallel" expression vectors. *Protein Expr Purif* **15**: 34–39.

Shimizu T, Ihara K, Maesaki R, Kuroda S, Kaibuchi K, Hakoshima T (2000) An open conformation of switch I revealed by the crystal structure of a Mg2+-free form of RHOA complexed with GDP. Implications for the GDP/GTP exchange mechanism. *J Biol Chem* **275**: 18311–1817.

Sidhu SS (2000) Phage display in pharmaceutical biotechnology. *Curr Opin Biotechnol* **11**: 610–616.

Sidhu SS (2001) Engineering M13 for phage display. *Biomol Eng* **18**: 57–63.

Sidhu SS, Lowman HB, Cunningham BC, Wells JA (2000) Phage display for selection of novel binding peptides. *Methods Enzymol* **328**: 333–363.

Sidhu SS, Fairbrother WJ, Deshayes K (2003) Exploring protein-protein interactions with phage display. *Chembiochem* **4**: 14–25.

Thapar R, Karnoub AE, Campbell SL (2002) Structural, biophysical insights into the role of the insert region in Rac1 function. *Biochemistry* **41**: 3875–3883.

Webb MR (1992) A continuous spectrophotometric assay for inorganic phosphate, for measuring phosphate release kinetics in biological systems. *Proc Natl Acad Sci USA* **89**: 4884–4887.

Wei Y, Zhang Y, Derewenda U, Liu X, Minor W, Nakamoto RK, Somlyo AV, Somlyo AP, Derewenda ZS (1997) Crystal structure of RhoA-GDP, its functional implications. *Nat Struct Biol* **4**: 699–703.

Zhang B, Wang ZX, Zheng Y (1997) Characterization of the interactions between the small GTPase Cdc42, its GTPase-activating proteins, putative effectors. Comparison of kinetic properties of Cdc42 binding to the Cdc42-interactive domains. *J Biol Chem* **272**: 21999–22007.

Zhang B, Zhang Y, Wang Z, Zheng Y (2000) The role of Mg^{2+} cofactor in the guanine nucleotide exchange, GTP hydrolysis reactions of Rho family GTP-binding proteins. *J Biol Chem* **275**: 25299–25307.